Evaluation of Phenomenological Characteristics of the Two-proton Decay of the ^{45}Fe Nucleus*

D. E. Lyubashevsky[1] S. G. Kadmensky[1] J. D. Shcherbina[1]

[1]Voronezh State University, Voronezh, 394018, Russia

Abstract: A Green-function formalism describing sequential and virtual two-proton (2p) radioactivity is developed on the basis of the multiparticle theory of one-proton decay. In the proposed approach, two-proton emission is treated as two consecutive one-proton transitions connected by the Green's function of the intermediate nucleus, allowing both on-shell and off-shell intermediate states to be consistently included. Analytical expressions are derived for the total and partial 2p-decay widths as well as for the angular distribution of the emitted protons. The formalism is applied to the ground-state two-proton decay of ^{45}Fe leading to the ground state of ^{43}Cr within the superfluid nuclear model. Calculations demonstrate a pronounced dependence of the decay characteristics on the choice of the single-particle nuclear potential. It is shown that an appropriate choice of the shell potential allows the experimental decay width and the measured proton angular distribution to be reproduced simultaneously. These results indicate that the proposed Green-function approach provides a consistent description of virtual sequential two-proton decay and offers an alternative framework for the interpretation of true two-proton radioactivity. The new elements of the work are: (i) a general Green-function formalism consistently including both on-shell and off-shell intermediate states; (ii) a natural separation of the total width into sequential and virtual contributions within a single framework; (iii) an extension of the formalism to deformed nuclei and to off-diagonal transitions in spherical nuclei; (iv) a simultaneous description of the total width and the proton angular distribution for 45Fe.

Keywords: two-proton radioactivity, Green-function formalism, superfluid nuclear model, proton angular distribution, Iron-45

DOI: **CSTR:**

CPC Accepted

I. INTRODUCTION

Two-proton (2p) radioactivity is one of the most intriguing decay modes of nuclei located beyond the proton drip line. Unlike one-proton (1p) emission, the 2p-decay process is governed not only by the properties of individual proton emission but also by correlations between the emitted protons and the structure of intermediate nuclear configurations. Consequently, the development of theoretical approaches capable of consistently describing different mechanisms of two-proton emission remains an important problem of modern nuclear physics.

The theoretical description of 1p radioactivity is well developed. The characteristics of 1p decays from ground and isomeric states of both spherical and deformed nuclei have been investigated experimentally in detail (see the review in Ref. [1]) and are successfully described within the framework of the multiparticle theory developed on the basis of the approaches originally proposed for α decay [2, 3]. This formalism has subsequently been extended to diagonal and off-diagonal one-proton decays [4-7] and employs integral expressions for calculating decay widths.

In the present work we develop a general Green-function formalism for two-step two-proton (2p) decay. In contrast to a direct three-body description, in which two-proton emission is treated as a simultaneous emission of two protons, we describe 2p decay as two successive one-proton transitions connected by the Green's function of the intermediate nucleus $(Z-1,A-1)$. In other words, the process is represented as the chain $(Z,A) \to (Z-1, A-1)+p_1 \to (Z-2,A-2)+p_1+p_2$,

where the first and second transitions are described by one-proton amplitudes, and the connection between them is provided by the Green's function of the intermediate nucleus.

This approach has several principal advantages. First, it allows both on-shell and off-shell intermediate states to be treated on equal footing. On-shell states correspond to a real one-proton decay of the intermediate nucleus and give rise to the sequential mechanism of 2p decay. Off-shell states cannot be realized as a real one-proton decay

Received 25 August 2026; Accepted 13 October 2026

* This work was supported by the Russian Science Foundation (Project No. 25-22-00697).

©2026 Chinese Physical Society and the Institute of High Energy Physics of the Chinese Academy of Sciences and the Institute of Modern Physics of the Chinese Academy of Sciences and IOP Publishing Ltd. All rights, including for text and data mining, AI training, and similar technologies, are reserved.

but contribute to the virtual mechanism. Second, the total 2p-decay width naturally separates into two contributions:

- a **sequential contribution** given by the residue at the pole of the Green's function of the intermediate nucleus;
- a **virtual contribution** associated with the principal-value integral along the real energy axis.

This separation is not introduced ad hoc but follows from the analytic properties of the Green's function. It allows both mechanisms of 2p decay to be described within a single formalism and their interrelation to be established.

Finally, since the formalism is formulated in terms of microscopic one-proton amplitudes, it naturally accounts for the structure of the initial, intermediate, and final nuclei: shell structure, angular-momentum coupling, pairing correlations, and superfluid effects. This distinguishes it from phenomenological approaches in which an effective three-body interaction is introduced or a diproton clustering is assumed.

Following the prediction of two-proton radioactivity by Goldansky [8], extensive experimental and theoretical studies of this decay mode have been carried out (see the review in Ref. [9]). Depending on the energetics of the intermediate nucleus, existing theoretical approaches distinguish two principal decay mechanisms: sequential and true two-proton emission.

Sequential two-proton decay corresponds to the emission of two protons in two successive one-proton transitions through real intermediate nuclear states, when both one-proton decay energies are positive.

Under these conditions, the interaction between the emitted protons can be neglected to a good approximation, and the decay can be described as two independent one-proton processes. Such an approach forms the basis of the R-matrix description of nuclear reactions involving unstable intermediate states [11] and of the kinetic-equation formalism for successive radioactive decays [12]. Sequential two-step decays of spherical nuclei were investigated in detail in Ref. [10].

In contrast, true two-proton radioactivity occurs when at least one of the one-proton decay channels is energetically closed, whereas the total two-proton decay energy remains positive. In this case, the decay proceeds via genuine three-body dynamics, which makes it impossible to represent the total decay width as a product of two independent one-proton amplitudes. We note from the outset that the present work neglects the interaction between the emitted protons after emission, as well as the p-p interaction in the virtual intermediate channel. This approximation is standard for the sequential mechanism, where the emissions are separated in time. Its justification and quantitative estimate are given in Sec. II and Sec. VI. Including p-p correlations would require a modification of the three-particle Green function and is beyond the scope of this work.

This problem has been successfully addressed within the hyperspherical three-body formalism developed in Refs. [13-15] and reviewed in Ref. [9], where both nuclear and Coulomb interactions between the three fragments are treated explicitly.

The first experimental observation of true two-proton radioactivity was reported for the ground-state decay of the ^{45}Fe nucleus [17, 18], confirming the earlier prediction of Ref. [16]. Since then, this nucleus has become one of the benchmark systems for investigations of two-proton emission. In addition to the total decay width [17, 18], measurements of the energy [19] and angular [20, 21] distributions of the emitted protons have provided stringent tests for theoretical models. While the diproton model based on the virtual ^{2}He state [22-25] was unable to reproduce the experimental observations satisfactorily, significantly better agreement was obtained within the three-body R-matrix approach [26]. Nevertheless, this description employs effective three-body interactions whose relation to the shell-model potentials and superfluid nucleon-nucleon interactions commonly used in nuclear-structure calculations remains an open question [26].

An alternative description of two-step two-proton decay was proposed in Refs. [27-29]. In that approach, the decay is represented as two successive one-proton emissions connected through the intermediate nucleus, and the corresponding decay widths are constructed from integral expressions for one-proton decay amplitudes [30-32]. The formalism employs conventional shell-model potentials together with the superfluid description of nucleon pairing. However, the previous formulation was restricted to the case of delayed sequential proton emission and did not explicitly include contributions associated with virtual intermediate configurations. Thus, compared with Ref. [10], the present work extends the formalism to deformed nuclei and to off-diagonal single-particle transitions in spherical nuclei, and explicitly includes virtual intermediate configurations that were not considered in [10]. Compared with Refs. [27-29], where the formulation was restricted to delayed sequential emission, the present approach allows both the sequential and the virtual mechanisms to be described within a single Green-function framework.

Among the continuum shell-model formulations, a fully microscopic treatment of two-proton emission was developed by Rotureau et al. [33] within the Shell Model Embedded in the Continuum (SMEC) framework. By explicitly partitioning the total Hilbert space into bound discrete configurations (Q), one-proton continuum ($\mathcal{P}$), and two-proton continuum ($\mathcal{T}$), SMEC provides a rigorous unified description of nuclear structure and reaction dynamics. Depending on the relative energy and coupling matrix elements between these subspaces, SMEC distinguishes three asymptotic modes of two-proton emission:

1. Direct emission via three-body asymptotics (or di-

CPC Accepted

proton cluster decay): Arising from direct transitions from the bound Q subspace to the two-particle continuum $\mathcal{T}$ via $H_{Q\mathcal{T}}G^{(+)}_{\mathcal{T}}H_{\mathcal{T}Q}$, and is effective when intermediate $A-1$ states are energetically closed ($\mathcal{P}$ -subspace coupling is suppressed).

2. Sequential decay through intermediate resonances: Proceeds via real intermediate resonance states in the $A-1$ nucleus embedded in the $\mathcal{P}$ subspace.

3. Virtual sequential decay through the correlated continuum: Proceeds through the off-shell continuum of the $A-1$ system in the absence of real, energetically accessible intermediate resonances.

While SMEC offers a comprehensive microscopic treatment including full configuration mixing and channel antisymmetrization, its practical implementation requires extensive multi-configuration shell-model calculations and effective zero-range residual interactions. In contrast, the Green-function formalism proposed in the present work constructs two-proton decay width directly from single-proton transition potentials and superfluid nucleon-nucleon pairing correlations, providing a computationally transparent alternative for describing both real on-shell and virtual off-shell intermediate transitions.

In the present work, we extend this approach by developing a general Green-function formalism for diagonal two-step two-proton decays of spherical and deformed nuclei in both ground and excited states. The proposed formulation consistently incorporates both on-shell and off-shell intermediate nuclear states through the Green's function of the intermediate nucleus. As a result, the total decay width is naturally separated into sequential and virtual contributions, providing a unified description of real and virtual two-step proton emission within the same theoretical framework. The formalism is applied to the ground-state two-proton decay of ^{45}Fe leading to the ground state of ^{43}Cr, where the total decay width and proton angular distribution are calculated within the superfluid model of the atomic nucleus [34].

I. FORMALISM OF SINGLE-PROTON DECAY

To formulate a general description of two-proton decay, we first briefly summarize the theoretical formalism of single-proton (1p) decay developed in Refs. [2-7, 10], which constitutes the basis of the present approach. We consider the decay of a spherical or deformed parent nucleus A from an arbitrary ground or excited state i, characterized by the center-of-mass momentum, total angular momentum, its projection, and additional quantum numbers. The wave function of the parent nucleus in the state i is written as

$$\psi_i = \frac{1}{\sqrt{L^3}} e^{\frac{i(\mathbf{P}_A \cdot R_A)}{\hbar}} \psi^{J_A m_A}_{\sigma_A} \tag{1}$$

where the first factor is the plane wave describing the center-of-mass motion of the parent nucleus, normalized to unity within a cubic volume with periodic boundary conditions, whereas the second factor represents the intrinsic wave function of the nucleus with internal energy. The latter is related to the binding energy of the parent nucleus by

$$E(Z,A,J_A,\sigma_A) = E_0(Z,A) + U(Z,A,J_A,\sigma_A), \tag{2}$$

where $E_0(Z,A)$ is the ground-state energy of the nucleus and $U(Z,A,J_A,\sigma_A)$ is its excitation energy. Accordingly, the total energy E_i of the parent nucleus is given by

$$E_i = E(Z,A,J_A,\sigma_A) + \frac{P_A^2}{2M_A}. \tag{3}$$

At 1p decays the nucleus (Z,A) passes from the initial state i to the final state $f = p_1 m_1 f_1$, corresponding to the ejected proton with momentum p_1 and its spin projection m_1 and to the state f_1 of the daughter nucleus $(Z-1,A-1)$ with wave function ψ_{f_1} and energy E_{f_1} defined by formulas (1) and (3) when index i is replaced by index $f_1 = \mathbf{P}_{A-1} J_{A-1} m_{A-1} \sigma_A$. 1, including momentum $\mathbf{P}_{A-1}$, center of mass of the daughter nucleus with coordinate $\mathbf{R}\,A-1$ and internal state of the daughter nucleus with wave function $\psi^{J_{A-1}m_{A-1}}_{\sigma_{A-1}}$ Introducing coordinates $\mathbf{R}_A, \mathbf{r}$ and momenta $\mathbf{P}_f, \mathbf{p}$, related to the initial coordinates $R_{A-1}, \mathbf{r}_1$ and momenta $\mathbf{P}_{A-1}, \mathbf{p}_1$ by the relations:

$$\begin{cases} \mathbf{r} = \mathbf{r}_1 - R_{A-1}, \\ \mathbf{R}_A = \dfrac{M_{A-1}R_{A-1} + m_p \mathbf{r}_1}{M_A}, \end{cases} \quad \begin{cases} \mathbf{P}_f = \mathbf{p}_1 + \mathbf{P}_{A-1}, \\ p = \dfrac{M_{A-1}\mathbf{p}_1 - M_p \mathbf{P}_{A-1}}{M_A}, \end{cases} \tag{4}$$

where M_p, M_A, M_{A-1} denote the masses of the proton, parent nucleus, and daughter nucleus, respectively, the wave function ψ_f of the final state can be written, following Refs. [2-7, 10], in the form

$$\psi_f = \frac{1}{\sqrt{L^3}} e^{\frac{i(\mathbf{P}_f \cdot R_A)}{\hbar}} \psi^{J_{A-1}m_{A-1}}_{\sigma_{A-1}} \varphi_{p_1}, \tag{5}$$

The proton wave function entering Eq. (5) is represented as

$$\varphi_{p_1} = \chi_{\frac{1}{2}m_1} \frac{1}{\sqrt{L^3}} \chi_k(\mathbf{r}), \tag{6}$$

where $\chi_{\frac{1}{2}m_1}$ is the proton spin function and $\chi_k(\mathbf{r})$ is the distorted wave describing the relative motion of the emitted proton and the daughter nucleus in the effective interaction potential. For diagonal 1p decays of spherical and deformed nuclei, this potential is determined by the spherical component of the Coulomb interaction between the proton and the daughter nucleus [2-5, 7]. For off-diagonal 1p decays of spherical nuclei, the effective interaction is described by the optical potential introduced in Ref. [6], which accounts for both nuclear and Coulomb

CPC Accepted

interactions.

In the following, we restrict ourselves to diagonal 1p decays of spherical and deformed nuclei and to off-diagonal decays of spherical nuclei only. Under these assumptions, the effective interaction becomes spherically symmetric, and the distorted wave can be expanded as

$$\chi_{\mathbf{k}}(\mathbf{r}) = 4\pi \sum_{lm_l} i^l \frac{\varphi_l(k,r)}{kr} Y_{lm_l}(\Omega_{\mathbf{r}}) Y^*_{lm_l}(\Omega_{\mathbf{k}}), \tag{7}$$

where the spherical Bessel functions $j_l(k,r)$ are replaced by the regular radial solutions $\frac{\varphi_l(k,r)}{kr}$ of the Schrödinger equation in the effective potential, satisfying the appropriate boundary conditions and containing the scattering phase shifts.

The total energy E_f of the final state is expressed as

$$E_f = E(Z-1, A-1, J_{A-1}, \sigma_{A-1}) + \frac{\mathbf{p}_1^2}{2m_p} + \frac{\mathbf{P}_{A-1}^2}{2M_{A-1}}, \tag{8}$$

Using the conservation of total energy together with Eqs. (3) and (8), one obtains

$$\begin{aligned} &Q_1(J_A, \sigma_A; J_{A-1}, \sigma_{A-1}) = \\ &\quad E(Z, A, J_A, \sigma_A) - E(Z-1, A-1, J_{A-1}, \sigma_{A-1}), \end{aligned} \tag{9}$$

which leads to

$$Q_1(J_A, \sigma_A, J_{A-1}, \sigma_{A-1}) = \frac{\mathbf{p}_1^2}{2M_p} + \frac{\mathbf{P}_{A-1}^2}{2M_{A-1}} - \frac{\mathbf{P}_A^2}{2M_A}, \tag{10}$$

Taking into account the coordinate transformation (4) and the conservation of total momentum,

$$P_A = P_f \tag{11}$$

Eq. (10) can be reduced to the form

$$Q_1(J_A, \sigma_A; J_{A-1}, \sigma_{A-1}) = \frac{\hbar^2 k^2}{2\mu_1} = T \tag{12}$$

where T is the kinetic energy of the relative proton-daughter motion and $\mu_1 = \frac{M_p M_{A-1}}{M_A}$ is the corresponding reduced mass.

Within the formalism developed in Refs. [2-7], the total width of the 1p decay of an unpolarized parent nucleus, averaged over the spin projections of the initial state, is given by

$$\Gamma^{J_A}_{p\sigma_A} = \frac{2\pi}{2J_A+1} \sum_{m_A f} \left| M_{fi} \right|^2 \delta(E_f - E_i), \tag{13}$$

where the transition matrix element M_{fi} is defined as

$$M_{fi} = \widehat{A} \left\{ \psi_f | \widetilde{V}_{\mathrm{p}_1 A-1} \rangle \right\} \psi_i, \tag{14}$$

with

$$\widetilde{V}_{\mathrm{p}_1 A-1} = \widetilde{V}^d_{\mathrm{p}_1 A-1}(\mathbf{r}) \equiv \mathrm{Re}\, V^{opt}_{\mathrm{p}_1 A-1}(\mathbf{r}) - \left(V^{coul}_{\mathrm{p}_1 A-1}(\mathrm{r}) \right)^0, \tag{15}$$

For diagonal 1p decays of spherical and deformed nuclei, the transition potential is determined by Eq. (15) [2-5, 7]. In the case of off-diagonal decays of spherical nuclei, it is expressed through the effective proton-nucleon interaction, which, within the theory of finite Fermi systems, coincides with the quasiparticle interaction amplitude in the particle-hole channel [6, 35].

It is convenient to introduce the channel function $U_c^{J_A m_A}$

$$U_c^{J_A m_A} = \sum_{m_{A-1} m_j m_l m_1} C^{J_A m_A}_{J_A - 1\, j m_{A-1} m_j} C^{j m_j}_{j \frac{1}{2} m_l m_1} Y_{l m_l}(\Omega_{\mathbf{r}}) \chi_{\frac{1}{2} m_1} \psi^{J_{A-1} m_{A-1}}_{\sigma_{A-1}} \tag{16}$$

where the channel quantum numbers specify the angular momentum coupling scheme. Using the properties of the Clebsch-Gordan coefficients, the final-state wave function $\psi^{J_{A-1} m_{A-1}}_{\sigma_{A-1}} \chi_{\frac{1}{2} m_1} \chi_{\mathbf{k}}(\mathbf{r})$(5) can be expanded as

$$\begin{aligned} &\psi^{J_{A-1} m_{A-1}}_{\sigma_{A-1}} \chi_{\frac{1}{2} m_1} \chi_{\mathbf{k}}(\mathbf{r}) = \\ &\quad 4\pi \sum_{l j m_l m_j} i^l \frac{\varphi_l(k,r)}{kr} Y^*_{l m_l}(\Omega_{\mathbf{k}}) C^{J_A m_A}_{J_{A-1} j m_{A-1} m_j} C^{j m_j}_{\frac{1}{2} m_l m_l} U_c^{J_A m_A}. \end{aligned} \tag{17}$$

Substituting Eq. (17) into Eq. (14) and integrating over the center-of-mass coordinate, the transition matrix element M_{fi} assumes the form

$$M_{fi} = \frac{4\pi}{\sqrt{L^3}} \delta_{P_A, \mathbf{P}_f} \frac{1}{k} M^{J_A m_A}_{\sigma_A}(J_{A-1}, m_{A-1}, \sigma_{A-1}, m_1, \mathbf{k}), \tag{18}$$

where

$$\begin{aligned} &M^{J_A m_A}_{\sigma_A}(J_{A-1}, m_{A-1}, \sigma_{A-1}, m_1, \mathbf{k}) = \\ &\quad \sum_{l j m_l m_j} i^l Y^*_{l m_l}(\Omega_{\mathbf{k}}) C^{J_A m_A}_{J_{A-1} j m_{A-1} m_j} C^{j m_j}_{l \frac{1}{2} m_l m_l} M^{J_A}_{\sigma_A c}(T), \end{aligned} \tag{19}$$

and the reduced matrix element $M^{J_A}_{\sigma_A c}(T)$ is given by

$$M^{J_A}_{\sigma_A c}(T) = \widehat{A} \left\{ U_c^{J_A m_A} \frac{\varphi_l(k,r)}{r} \mid \widetilde{V}_{\mathrm{p}_1 A-1} \right\} \mid \psi^{J_A m_A}_{\sigma_A}. \tag{20}$$

Substituting Eq. (18) into Eq. (13), replacing the summation over the proton momentum by integration, and using the energy conservation relation (12), one arrives at

CPC Accepted

the following expression for the total 1p-decay width:

$$\Gamma^{J_A}_{p\sigma_A} = \frac{2\pi}{(2J_A+1)} \sum_{m_A m_{A-1} m_1 J_{A-1}\sigma_{A-1}} \int \left| \sum_{ljm_l m_j} i^l C^{J_A m_A}_{J_{A-1} j m_{A-1} m_j} C^{jm_j}_{l\frac{1}{2}m_l m_l} Y^*_{lm_l}(\Omega_{\mathbf{k}}) \widetilde{M}^{J_A}_{\sigma_A c}(T) \right|^2 d\Omega_{\mathbf{k}}, \quad (21)$$

where the reduced transition matrix element is determined by Eq. (20), with the regular Coulomb radial function replaced by the energy-normalized scattering solution.

Finally, summation over the angular-momentum projections m_A, m_{A-1}, m_1 using the orthogonality of the Clebsch-Gordan coefficients yields the isotropic angular distribution of protons emitted from an unpolarized parent nucleus. Accordingly, the total width can be represented as the sum of partial widths $\Gamma^{J_A}_{p\sigma_A c}(T)$,

$$\Gamma^{J_A}_{p\sigma_A} = \sum_c 2\pi \left| \widetilde{M}^{J_A}_{\sigma_A c}(T) \right|^2 \int \frac{d\Omega_{\mathbf{k}}}{4\pi} = \sum_c \Gamma^{J_A}_{p\sigma_A c}(T). \quad (22)$$

where the partial proton widths $\Gamma^{J_A}_{p\sigma_A c}(T)$ are determined by the integral expression previously derived in Refs. [2-7]:

$$\Gamma^{J}_{p\sigma_{A^c} c}(T) = 2\pi \left| \widetilde{M}^{J_A}_{\sigma_{A^c} c}(T) \right|^2. \quad (23)$$

II. FORMALISM OF TWO-STEP TWO-PROTON DECAY

Following the single-proton formalism summarized in Sec. I and developed in Refs. [2-7, 10], we now derive a general expression for the width of two-step two-proton (2p) decay. We consider the transition of a spherical or deformed parent nucleus from the initial state (i), described by the wave function $\psi_i(1)$ and energy $E_i(3)$, to the final state $f = \mathbf{p}_1 m_1 \mathbf{p}_2 m_2$, characterized by

$$E_f = \frac{\mathbf{p}_1^2}{2m_p} + \frac{\mathbf{p}_2^2}{2m_p} + \frac{\mathbf{P}^2_{A-2}}{2m_{A-2}} + E(Z-2, A-2, J_{A-2}, \sigma_{A-2}), \quad (24)$$

associated with the emission of the first and second protons with coordinates, momenta, and projections of spins $\mathbf{r}_1, \mathbf{p}_1, m_1$ and $\mathbf{r}_2, \mathbf{p}_2, m_2$, respectively, and the formation of a final nucleus $(Z-2, A-2)$ in a state f_2 with wave function ψ_{f_2} and energy E_{f_2}, defined by formulas (9) and (10) when the index i is replaced by the index f_2. In the following, we restrict ourselves to the cases in which the dominant contribution to the two-step decay arises from diagonal one-proton decays of spherical and deformed nuclei and from one-proton decays involving off-diagonal matrix elements for spherical nuclei. Under these assumptions, the two-step decay width of an unpolarized parent nucleus, averaged over the spin projections of the initial state, can be written in the same form as Eq. (13), with the transition matrix element M_{fi} represented diagrammatically in Fig. 1.

In Fig. 1, the filled circles denote the vertex functions describing the interaction of the emitted proton with the residual nucleus through the effective transition potential $\widetilde{V}_{\mathrm{p},A-1}$, whereas the bold directed line represents the one-particle Green's function $G(Z-1, A-1)$ of the intermediate nucleus $(Z-1, A-1)$,

$$G(Z-1, A-1) = \sum_{f_1} \frac{|\psi_{f_1}\psi_{f_1}|}{E_i - E_{f_1} - \frac{\mathbf{p}_1^2}{2m_p} + \frac{i\Gamma^{J_{A-1}}_{\sigma_{A-1}}}{2}}, \quad (25)$$

where the finite total width $\Gamma^{J_{A-1}}_{\sigma_{A-1}}$ of the intermediate nuclear state $J_{A-1}\sigma_{A-1}$ is explicitly taken into account. The

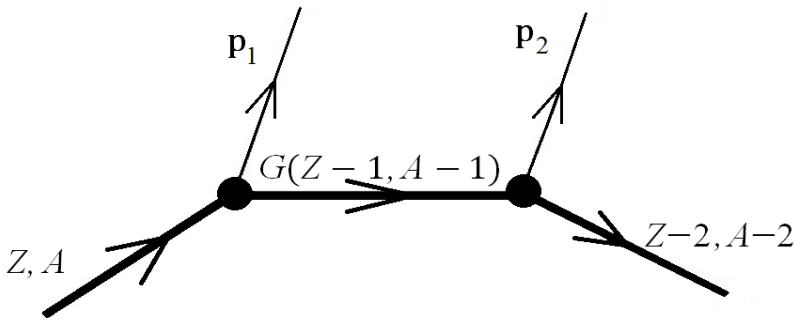

Fig. 1. Diagram illustrating the process of two-step two-proton decay. Here, (Z,A) and $(Z-2,A-2)$ stand for the charges and masses of initial and final nuclei, p1 and p2 are the momenta of emitted protons, and $G(Z-1,A-1)$ is the Green's function for the intermediate nucleus.

CPC Accepted

present formalism assumes that the width of the intermediate state considerably exceeds the total width of the initial parent $(Z-1,A-1)$ state. This condition is naturally fulfilled, for example, for ground-state two-proton decay of even Z nuclei, where proton pairing results in substantially different one-proton decay energies of the parent and intermediate nuclei [10].

To substantiate the assumption that the width of the intermediate state of $\Gamma^{J_{A-1}}_{\sigma_{A-1}}$ significantly greater than the width of the parent nucleus $\Gamma^{J_A}_{\sigma_A}$, let us estimate the value of $\Gamma^{J_{A-1}}_{\sigma_{A-1}}$ for the nucleus ^{44}Mn within the framework of the same superfluid model. Using formula (23) and the corresponding single-particle amplitudes, we obtain $\Gamma^{J_{A-1}}_{\sigma_{A-1}} \sim 10^{-16} - 10^{-15}$MeV (depending on the potential), which is $2-3$ orders of magnitude greater than $\Gamma^{J_A}_{\sigma_A} \sim 10^{-19}$MeV. Consequently, the condition $\Gamma^{J_{A-1}}_{\sigma_{A-1}} \gg \Gamma^{J_A}_{\sigma_A}$ is fulfilled with a large margin, and neglecting the width of the parent state in the denominator of the Green function is correct. Before proceeding, we estimate the accuracy of neglecting the p-p interaction. For 45Fe at a typical energy of about 1MeV and Z = 26, the Coulomb correction to the total width is a few percent. This is significantly smaller than the observed sensitivity of the results to the choice of the single-particle potential, which reaches a factor of 10-20 (see Sec. IV). In the sequential channel, the interaction between the protons is further suppressed by the time separation between the emissions. As for the virtual channel, including the p-p interaction would require constructing a three-particle Green-function with explicit pairing correlations in the continuum, which is beyond the scope of this work. Thus, neglecting the p-p interaction is a controlled approximation in the energy and mass range considered.

Moreover, taking into account the finite width of $\Gamma^{J_A}_{\sigma_A}$ would lead to corrections of the order $\Gamma^{J_A}_{\sigma_A}/\Gamma^{J_{A-1}}_{\sigma_{A-1}} \sim 10^{-3}$, which lies far beyond the accuracy of our calculation.

The intermediate state $f_1 = \mathbf{P}_{A-1}J_{A-1}m_{A-1}\sigma_{A-1}$ entering Eq. (25) is described by the wave function and energy obtained from Eqs. (1) and (3) after replacing the index i with f_1. Using the energy relation (9), the denominator of the Green's function can be rewritten accordingly.

Depending on its energy, the intermediate nuclear state may correspond either to a real or to a virtual configuration. When the intermediate state satisfies the energy E_{f_1} conservation law $E_{f_1} + \frac{\mathbf{p}_1^2}{2M_p} = E_i$,

$$T = Q_1(J_A,\sigma_A;J_{A-1},\sigma_{A-1}), \tag{26}$$

it lies on the mass shell of the decaying system and corresponds to a real one-proton decay of the parent nucleus. This situation gives rise to the sequential two-step two-proton decay mechanism. Conversely, if Eq. (26) cannot be fulfilled for any physically accessible energy, the intermediate state remains off shell and contributes only virtually, leading to the virtual two-step two-proton decay mechanism.

To evaluate the corresponding decay width, we introduce the relative coordinates momenta $\mathbf{r},\mathbf{p}$ and $\mathbf{r}',\mathbf{p}'$ of the proton-nucleus subsystems by transformations analogous to Eq. (4). Applying the conservation of energy $E_f = E_i$ together with Eqs. (3) and (24), we obtain

$$Q_0(J_A,\sigma_A;J_{A-2},\sigma_{A-2}) = \frac{\mathbf{p}^2}{2\mu_1} + \frac{\mathbf{p}'^2}{2\mu_2} = T + T', \tag{27}$$

where the total two-proton decay energy $Q_0(J_A,\sigma_A;J_{A-2},\sigma_{A-2})$ is expressed as

$$\begin{aligned} &Q_0(J_A,\sigma_A;J_{A-2},\sigma_{A-2}) \\ &= E(Z,A,J_A,\sigma_A) - E(Z-2,A-2,J_{A-2},\sigma_{A-2}) \\ &= Q_1(J_A,\sigma_A;J_{A-1},\sigma_{A-1}) + Q_2(J_{A-1},\sigma_{A-1};J_{A-2},\sigma_{A-2}) \end{aligned} \tag{28}$$

and the remaining quantities denote the reduced mass μ_2 and kinetic energy T' of the second proton relative to the final nucleus $(Z-2,A-2)$.

Using distorted proton wave functions $\bar{V}_{\mathrm{p}_1A-1}(\mathbf{r})$ and $\bar{V}_{\mathrm{p}_2A-2}(\mathbf{r})$ of the form introduced in Eq. (7), together with channel expansions analogous to Eq. (17), replacing the momentum summation by integration and applying the energy conservation relation (27), the general expression for the two-step two-proton decay width corresponding to the diagram shown in Fig. 1 becomes

$$\begin{aligned} \Gamma^{J_A}_{2p\sigma_A} = \frac{2\pi}{2J_A+1} \sum_{m_A m_1 m_2 m_{A-2} J_{A-2}\sigma_{A-2}} & Q_0(J_A,\sigma_A;J_{A-2},\sigma_{A-2})dT\times \\ \times \left| \int_{J_{A-1}\sigma_{A-1}m_{A-1}} \frac{\widetilde{M}^{J_A m_A}_{\sigma_A}(J_{A-1},m_{A-1},\sigma_{A-1},m_1,\mathbf{k})\widetilde{M}^{J_{A-1}m_{A-1}}_{\sigma_{A-1}}(J_{A-2},m_{A-2},\sigma_{A-2},m_2,\mathbf{k}')}{Q_1(J_A,\sigma_A;J_{A-1},\sigma_{A-1}) - T + \frac{i\Gamma^{J_{A-1}}_{\sigma_{A-1}}}{2}} \right|^2 & d\Omega_{\mathbf{k}}d\Omega_{\mathbf{k}'}, \end{aligned} \tag{29}$$

where the wave numbers of the emitted protons are determined from

$$T = \frac{\hbar^2k^2}{2\mu_1},\ T' = \frac{\hbar^2k^2}{2\mu_2} = Q_0(J_A,\sigma_A;J_{A-2},\sigma_{A-2}) - T, \tag{30}$$

Chin. Phys. C Accepted

and the matrix elements $\widetilde{M}^{J_A m_A}_{\sigma_A}(J_{A-1}, m_{A-1}, \sigma_{A-1}, m_1, \mathbf{k})$ and $\widetilde{M}^{J_{A-1} m_{A-1}}_{\sigma_{A-1}}(J_{A-2}, m_{A-2}, \sigma_{A-2}, m_2, \mathbf{k}')$ are obtained from Eq. (19) after replacing the index $J_{A-1}\sigma_{A-1} l m_l j m_j$ by the $J_{A-1}\sigma_{A-1} l_1 m_{l_1} j_1 m_{j_1}$ and $J_{A-2}\sigma_{A-2} l_2 m_{l_2} j_2 m_{j_2}$, respectively.

In deriving Eq. (29) we neglect the interaction between the emitted protons. This means that the effective potentials $V_{p1\,A^{-1}}$ and $V_{p2\,A^{-2}}$ include only the interaction of each proton with the residual nucleus, while the p-p Coulomb interaction after emission and p-p correlations in the virtual channel are not included. The justification and accuracy estimate of this approximation are given below.

Integration of Eq. (29) over the emission directions of both protons, followed by the use of the completeness and orthogonality relations of the Clebsch-Gordan coefficients, yields the total two-proton decay width in the form

$$\Gamma^{J_A}_{2p\sigma_A} = \frac{1}{2\pi} \sum_{JA-1\sigma_{A-1}J_{A-2}\sigma_{A-2}j_1 l_1 j_2 l_2} \times\times \int_0^{Q_0(J_A,\sigma_A;J_{A-2},\sigma_{A-2})} dT \frac{\Gamma^{J_A}_{p_1\sigma_A J_{A-1}\sigma_{A-1} j_1 l_1}(T)\Gamma^{J_{A-1}}_{p_2\sigma_{A-1}J_{A-2}\sigma_{A-2} j_2 l_2}(Q_0 - T)}{\left(Q_1(J_A,\sigma_A;J_{A-1},\sigma_{A-1})^2 + \frac{\left(\Gamma^{J_{A-1}}_{\sigma_{A-1}}\right)^2}{4}\right]}, \tag{31}$$

where the partial one-proton widths are defined by expressions analogous to Eq. (22).

For nuclei heavier than the lightest proton emitters, the total width of the intermediate state is generally much smaller than the corresponding decay energy $|Q_1|$. Under this condition, the integral appearing in Eq. (31),

$$I = \frac{1}{2\pi}\int_0^{Q_0} dT \Gamma^{J_A}_{p_1\sigma_A J_{A-1}\sigma_{A-1} j_1 l_1}(T)\Gamma^{J_{A-1}}_{p_2\sigma_{A-1}J_{A-2}\sigma_{A-2} j_2 l_2}(Q_0 - T)\left[(Q_1 - T)^2 + \frac{\left(\Gamma^{J_{A-1}}_{\sigma_{A-1}}\right)^2}{4}\right]^{-1} \equiv\equiv \frac{1}{2\pi}\int_{C_1} f(T)dT \tag{32}$$

can be evaluated by analytic continuation into the complex energy plane. Let us examine the analytic properties of the integrand $f(T)$ defined in Eq. (32). In the upper half-plane of the complex variable T, the function $f(T)$ is analytic everywhere except for a pole whose position is determined by the one-proton decay energy of the intermediate nucleus. For $Q_1 > 0$, the pole is located at $T = Q_1 + i\Gamma/2$ and lies in the upper half-plane. Closing the integration contour $C = C_1 + C_2$ in the upper half-plane, where C_1 runs along the real axis and C_2 is a semicircle of infinite radius, we obtain a decomposition of the integral into two contributions. The first is given by the residue at the pole and represents the sequential mechanism. The second, given by the principal-value integral along the real axis, represents the virtual mechanism. For $Q_1 < 0$, the pole does not lie on the physical contour, and only the virtual contribution remains. The integration contour C_1 is closed in the upper half-plane C_2 as illustrated in Fig. 2.

The integral I(32) may then be decomposed into two contributions,

$$I = I_1 + I_2 \tag{33}$$

where

$$I_1 = \frac{1}{2\pi}\oint_C f(T)dT,\ I_2 = -\frac{1}{2\pi}\int_{C_2} f(T)dT. \tag{34}$$

Application of Cauchy's residue theorem gives

$$I_1 = \frac{\Gamma^{J_A}_{p_1\sigma_A J_{A-1}\sigma_{A-1} j_1 l_1}(Q_1)\Gamma^{J_{A-1}}_{p_2\sigma_{A-1}J_{A-2}\sigma_{A-2} j_2 l_2}(Q_2)}{\Gamma^{J_{A-1}}_{\sigma_{A-1}}}, \tag{35}$$

Substitution of Eq. (35) into Eq. (31) leads to

$$\left(\Gamma^{J_A}_{2p\sigma_A}\right)^{suc} = \sum_{JA-1\sigma_{A-1}J_{A-2}\sigma_{A-2}j_1 l_1 j_2 l_2} \frac{\Gamma^{J_A}_{p_1\sigma_A J_{A-1}\sigma_{A-1} j_1 l_1}(Q_1)\Gamma^{J_{A-2}}_{p_2\sigma_{A-1}J_{A-2}\sigma_{A-2} j_2 l_2}(Q_0 - Q_1)}{\Gamma^{J_{A-1}}_{\sigma_{A-1}}}, \tag{36}$$

which represents the width of the sequential two-step two-proton decay associated with two successive real one-proton emissions.

The remaining contribution corresponds to the principal-value part of the integral. When the dominant contribution $|Q_1 - T| \gg \frac{\Gamma^{J_{4-1}}_{\sigma_{4-1}}}{2}$ arises from energies sufficiently far from the pole $T_0 = Q_1 + \frac{i\Gamma^{J_{A-1}}_{\sigma_{A-1}}}{2}$, the integral takes the form

CPC Accepted

$$I_2 = \frac{1}{2\pi}\int_0^{Q_0} dT\Gamma^{J_A}_{p_1\sigma_A J_{A-1}\sigma_{A-1} j_1 l_1}(T)\Gamma^{J_{A-1}}_{p_2\sigma_{A-1} J_{A-2}\sigma_{A-2} j_2 l_2}(Q_0 - T)[Q_1 - T]^{-2}. \quad (37)$$

The second contribution I_2 is the principal-value integral along the real axis. It is this contribution that we identify with the virtual mechanism of two-step 2p decay. This identification is unambiguous: the residue at the pole exhausts the sequential mechanism, while the remaining part of the integral, not associated with the pole, corresponds to off-shell intermediate configurations. For $Q_1 < 0$, the pole leaves the physical contour and I_1 vanishes, so that only the virtual contribution I_2 remains. Substituting Eq. (37) into Eq. (31) yields the width of the virtual two-step two-proton decay,

$$\left(\Gamma^{J_A}_{2p\sigma_A}\right)^v = \sum_{J_{A-1}\sigma_{A-1}J_{A-2}\sigma_{A-2}j_1 l_1 j_2 l_2} \frac{1}{2\pi}\int_0^{Q_0} dT\Gamma^{Q_0}_{p_1\sigma_A J_{A-1}\sigma_{A-1} j_1 l_1}(T)\Gamma^{J_{A-1}}_{p_2\sigma_{A-1} J_{A-2}\sigma_{A-2} j_2 l_2}(Q_0 - T)\times\times[(Q_1 - T)]^{-2} \quad (38)$$

Accordingly, when both one-proton decay energies Q_1 and Q_2Q_2 are positive, the total two-proton decay width is given by

$$\Gamma^{J_A}_{2p\sigma_A} = \left(\Gamma^{J_A}_{2p\sigma_A}\right)^{suc} + \left(\Gamma^{J_A}_{2p\sigma_A}\right)^{v}. \quad (39)$$

i.e., as the sum of the sequential and virtual contributions. If one of the one-proton decay energies becomes negative while the total two-proton decay energy remains positive, only the virtual contribution survives.

The expressions obtained for the sequential and virtual decay widths are identical in form to those derived previously for diagonal two-step decays of spherical nuclei in Ref. [10], but are now extended to include diagonal decays of deformed nuclei and transitions involving off-diagonal matrix elements in spherical nuclei. Consequently, the previously established correspondence between the sequential component and the results of the R-matrix theory [11] and the kinetic-equation approach [12] remains valid in the more general formulation developed here.

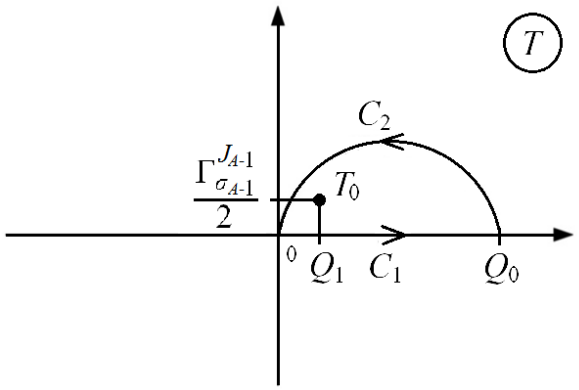

Fig. 2. Integration contour in the complex energy plane. The contour C_1 along the real axis is completed by the semicircular contour C_2, forming the closed contour $C = C_1 + C_2$. For positive values of the one-proton decay energy Q_1, the integrand possesses a pole $T = T_0 = Q_1 + \frac{i\Gamma^{J_{A-1}}_{\sigma_{A-1}}}{2}$ inside the contour.

Furthermore, as shown in Ref. [10], the expression for the virtual contribution is qualitatively consistent with the quasiclassical result obtained within the hyperspherical three-body formalism [15] when the interaction between the emitted protons is neglected.

Finally, adopting the quasiclassical approximation for deep sub-barrier one-proton decay widths [8], the relative magnitudes of the sequential and virtual contributions can be analyzed. As demonstrated in Ref. [10], sufficiently small values of the one-proton decay energy lead to a pronounced enhancement of the virtual contribution, which may exceed the sequential component.

The agreement of the obtained expressions in form with the results of Ref. [10] in the diagonal spherical limit is a consistency check of the formalism, not evidence of a lack of novelty. The new formalism also includes deformed nuclei, off-diagonal matrix elements, and an explicit treatment of virtual intermediate configurations. We emphasize that the developed formalism does not reduce to a purely independent single-particle calculation. It accounts for:

- the shell structure of the initial, intermediate, and final nuclei;
- angular-momentum coupling and selection rules;
- pairing correlations and superfluid effects;
- spectroscopic (genealogical) overlap factors;
- the Green's function of the intermediate nucleus with finite width.

These elements distinguish the present approach from a simple combination of two barrier penetrabilities with an energy denominator.

III. TOTAL AND PARTIAL WIDTHS OF DIAGONAL TWO-PROTON TWO-STEP VIRTUAL DECAYS OF SPHERICAL NUCLEI IN THE SUPERFLUID MODEL OF THE NUCLEUS

To illustrate the formalism developed in the preceding section, we consider the diagonal two-step two-pro-

CPC Accepted

ton decay of a spherical parent nucleus (Z,A) within the framework of the superfluid nuclear model [34] and the approach developed in Refs. [27-29]. By the superfluid model we mean the BCS model of the atomic nucleus with proton pairing correlations. In this model, the single-particle energies $E(j)$ and the occupation coefficients u_j, v_j are determined from the Bogoliubov equations. The quantities C_Z and λ_Z denote the correlation function and the chemical potential of the proton subsystem, and G is the pairing interaction parameter. The parameterization used follows Ref. [34]. The parent nucleus is assumed to decay from its ground state $J_A\sigma_A$ characterized by the quantum numbers and the corresponding intrinsic configuration. The decay is treated as two successive one-proton emissions.

During the first step, a proton occupying the shell-model orbital nlj is emitted from the parent nucleus, resulting in the formation of an intermediate nucleus. In the second step, another proton is emitted from the same orbital of the intermediate nucleus, leading to the ground state of the final nucleus. Within this approximation, the total width of the diagonal two-proton decay is expressed as the sum of the corresponding partial contributions [27-29],

$$\Gamma = \sum_{J_{A-1}\sigma_{A-1}nlj} \Gamma(J_A\sigma_A \to J_{A-1}\sigma_{A-1}, nlj \to J_{A-2}\sigma_{A-2}) \quad (40)$$

where the quantities $\Gamma(J_A\sigma_A \to J_{A-1}\sigma_{A-1}, nlj \to J_{A-2}\sigma_{A-2})$ denote the partial widths of the first and second one-proton transitions, respectively.

The partial widths depend on the kinetic energies of the emitted protons T_1 and $T_2 = \{Q_0(J_A\sigma_A; J_{A-2}\sigma_{A-2}) - T_1\}$, which are determined from the corresponding energy balance relations,

$$\Gamma(J_A\sigma_A \to J_{A-1}\sigma_{A-1}, nlj \to J_{A-2}\sigma_{A-2}) = \\ = \frac{1}{2\pi}\int_0^{Q_0(J_A\sigma_A;J_{A-2}\sigma_{A-2})} dT_1 \sum_{J_{A-1}\sigma_{A-1}} \left| \frac{\sqrt{\Gamma^A_{p_1}(J_A\sigma_A \to J_{A-1}\sigma_{A-1}, nlj)} \cdot \sqrt{\Gamma^{A-1}_{p_2}(J_{A-1}\sigma_{A-1} \to J_{A-2}\sigma_{A-2}, nlj)}}{Q_1(J_A\sigma_A; J_{A-1}\sigma_{A-1}) - T_1} \right|^2 \quad (41)$$

The one-proton decay energies $Q_1(J_A\sigma_A; J_{A-1}\sigma_{A-1})$ and $Q_2(J_{A-1}\sigma_{A-1}; J_{A-2}\sigma_{A-2})$ entering Eq. (41), together with the total two-proton decay energy $Q_0(J_A\sigma_A; J_{A-2}\sigma_{A-2})$, are expressed through the ground-state energies of the parent $E_0(J_A\sigma_A)$, intermediate Eq.(42-44), and final $E_0(J_{A-2}\sigma_{A-2})$ nuclei according to

$$Q_1(J_A\sigma_A; J_{A-1}\sigma_{A-1}) = E_0(J_A\sigma_A) - E(J_{A-1}\sigma_{A-1}) \quad (42)$$

$$Q_2(J_{A-1}\sigma_{A-1}; J_{A-2}\sigma_{A-2}) = E(J_{A-1}\sigma_{A-1}) - E_0(J_{A-2}\sigma_{A-2}), \quad (43)$$

$$Q_0(J_A\sigma_A; J_{A-2}\sigma_{A-2}) = E_0(J_A\sigma_A) - E_0(J_{A-2}\sigma_{A-2}). \quad (44)$$

The amplitudes determining the deep sub-barrier one-proton decay widths are calculated using the integral formalism developed in Refs. [30-32],

$$\sqrt{\Gamma^A_{p_1}(J_A\sigma_A \to J_{A-1}\sigma_{A-1}, nlj)} = \\ \sqrt{2\pi} \cdot G^A_{nlj} \int_0^\infty \widetilde{F}_l(k_1, r) V_{pA-1}(r) R_{nlj}(r) dr \quad (45)$$

where $\widetilde{F}_l(k_1, r)$ is the energy-normalized radial Coulomb wave function of the emitted proton, V_{pA-1} is the effective proton-nucleus interaction potential, and q is the parameter used to adjust the depth of the single-particle potential in calculations of one- and two-proton decay characteristics.

The single-particle potential is taken in the Woods-Saxon form adopted in Refs. [36-38], which has previously been shown to provide a satisfactory description of spherical nuclei over a broad range of proton and neutron numbers and has been successfully applied to the description of one-proton radioactivity in Refs. [31, 32]:

$$V_N = \frac{-|V_0|}{1+\exp\left[\frac{r-R_0}{a}\right]}, \; V_{ls} = -\frac{\chi}{r} \cdot \frac{dV_N(r)}{dr}(\mathbf{l}\cdot\mathbf{s}), R_0 = r_0 A^{1/3}, \quad (46)$$

The corresponding parameter values are listed in Table 1.

The radial single-particle wave function of the proton occupying the shell-model state nlj satisfies the Schrödinger equation

$$\left[-\frac{\hbar^2}{2m}\frac{d^2R_{nlj}(r)}{dr^2} + \frac{\hbar^2}{2m}\frac{l(l+1)}{r^2} + V_{pA-1}(r) + V^{coul}_{pA-1}(r)\right] R_{nlj}(r) \\ = E(j) R_{nlj}(r), \quad (47)$$

CPC Accepted

Table 1. Parameters of nuclear potentials.

Potential	V_0, MeV	r_0, Fm	χ, Fm^2	a, Fm
[36]	51.9+29.0(N-Z)/A	1.28	0.175	0.67
[37]	54.0+24.0(N-Z)/A	1.17	12.4/V	0.75
[38]	53.0+33.4(N-Z)/A	1.24	0.26·[1+2(N-Z)/A]	0.63

Where $V^{\text{coul}}_{pA-1}(r)$ the Coulomb interaction between the proton and the daughter $(Z-1,A-1)$ nucleus is included explicitly.

The one-proton decay amplitudes also contain the proton spectroscopic (genealogical) factor G^A_{nlj},

$$G^A_{nlj}(J_{P_A}\sigma_{P_A};J_{P_{A-1}}\sigma_{P_{A-1}},nlj) = \langle\left\{\psi^{J_{P_{A-1}}m_{P_{A-1}}}_{\sigma_{P_{A-1}}}a_{nljm}\right\}_{J_{P_A}m_{P_A}}|\psi^{J_{P_A}m_{P_A}}_{\sigma_{P_A}}\rangle, \quad (48)$$

which determines the overlap between the parent $\psi^{J_{P_A}m_{P_A}}_{\sigma_{P_A}J_{P_A}m_{P_A}}$ and daughter $\psi^{J_{P_{A-1}}m_{P_{A-1}}}_{\sigma_{P_{A-1}}J_{P_{A-1}}m_{P_{A-1}}}$ nuclear wave functions. For even- and odd- Z nuclei within the superfluid nuclear model, this quantity is given by [34]

$$G^{Ai}_{nlij} = +\sqrt{(21)}\,(Z\text{-even}),\ G^{A-1}_{nlj} = u^f_j\ (Z\text{-odd}). \quad (49)$$

The nuclear structure calculations are performed within the superfluid model of atomic nuclei [34]. For even- Z nuclei, the ground-state energy $E_{P_0}(J_A\sigma_A)$ and the corresponding Bogoliubov equations are written as

$$\frac{G}{2}\sum_j\frac{\left(j+\frac{1}{2}\right)}{\varepsilon(j)} = 1 \quad (50)$$

$$E_{P_0}(J_A\sigma_A) = \sum_j(2j+1)E(j)v^2_j - \frac{C^2_Z}{G}, \quad (51)$$

where

$$\varepsilon(j) \equiv \sqrt{C^2_Z + \{E(j)-\lambda_Z\}^2} \quad (52)$$

The quantities v_j, u_j denote the Bogoliubov transformation coefficients,

$$v^2_j = \frac{1}{2}\left\{1-\frac{E(j)-\lambda_Z}{\varepsilon(j)}\right\}, u^2_j = 1-v^2_j, \quad (53)$$

while the pairing interaction parameter G is expressed as [34]

$$G = \frac{A_0}{A} \quad (54)$$

where coefficient $A_0 = 16.5-17.5$, and C_Z and λ_Z are the correlation function and chemical potential of the proton subsystem.

For nuclei with an odd number of protons Z (the total spin of an odd proton is equal to j_2), the blocking effect of the unpaired proton modifies the corresponding equations. In this case, the ground-state energy E_P and the Bogoliubov equations take the form

$$\frac{G}{2}\left\{\sum_{j\neq j_2}\frac{j+1/2}{\varepsilon(j,j_2)}+\frac{j-1/2}{\varepsilon(j_2,j_2)}\right\} = 1 \quad (55)$$

$$Z = 1+(2j_2-1)v^2_j(j_2)+\sum_{j\neq j_2}(2j+1)v^2_j(j_2) \quad (56)$$

$$E_P = E(j_2)+(2j_2-1)E(j_2)v^2_j(j_2) + \sum_{j\neq j_2}(2j+1)E(j)v^2_j(j_2) - \frac{C^2_Z(j_2)}{G}, \quad (57)$$

$$\varepsilon(j,j_2) \equiv \sqrt{C^2_Z(j_2)+\{E(j)-\lambda_Z(j_2)\}^2}, \quad (58)$$

$$v^2_j(j_2) = \frac{1}{2}\left\{1-\frac{E(j)-\lambda_Z(j_2)}{\varepsilon(j,j_2)}\right\}; u^2_j(j_2) = 1-v^2_j(j_2). \quad (59)$$

The numerical part of the work illustrates the application of the developed formalism and demonstrates its sensitivity to the choice of the single-particle potential. It does not substitute for the theoretical novelty of the formalism but serves as a test in the limiting case already studied previously.

IV. CALCULATION OF TOTAL AND PARTIAL WIDTHS OF DIAGONAL TWO-STEP TWO-PROTON DECAY OF ^{45} FE NUCLEUS

The energies of one-proton decays (42) and (43) with proton escape and for the ground states of the parent and intermediate nucleus and 2p decay (44) can be found using the binding energies of the ground states of ^{45}Fe, ^{44}Mn, ^{43}Cr nuclei: $E_0(Z,A) = (-329.308\pm0.078)$MeV, $E_0(Z-1,A-1) = (-329.284\pm0.076)$MeV, $E_0(Z-2, A-2) = (-330.462\pm0.052)$MeV. As a result, the energies (3-5) calculated using the isospin symmetry property of nuclei [38] are defined as $Q_1 = (-0.024\pm0.109)$MeV, $Q_2 = (1.178\pm0.92)$MeV, and $Q_0 = (1.154\pm0.142)$MeV. The obtained energy value Q_0 is in the range of experimental values $Q^{\text{exp}}_0 = (1.154\pm0.016)$MeV [17-18], which will be used in further calculations. At the same time, the obtained value $Q_1 = (-0.024\pm0.109)$MeV, $Q_2 = (1.178\pm 0.92)$ and $Q_0 = (1.154\pm0.142)$. In principle, this leads to

CPC Accepted

the possibility of the occurrence of real one-proton decay for positive values lying in the found interval $0 \le Q_1 \le 0.085$MeV. Since the experimental energy distributions of emitted protons, in principle, do not indicate the possibility of the existence of this real one-proton decay, in further calculations for the value Q_1 will be used a negative value $Q_1 = -0.024$MeV, which weakly affects the calculated values of the total and partial widths of the 2p decay of the ^{45}Fe nucleus.

In calculations of the 2p decay widths, we fitted the energies $Q_1(J_A\sigma_A; J_{A-1}\sigma_{A-1})$ and $Q_0(J_A\sigma_A; J_{A-2}\sigma_{A-2})$ of both one-proton and 2p decays according to formulas (3-5) to their numerical values obtained above by varying the depth of the nuclear potential $V_{pA-1}(r)$ (through a change in the parameter q) and the superfluid parameter G. Table 2 shows the shell energies of the ^{45}Fe nucleus calculated for nuclear potentials [36-38] without fitting, and Table 3 shows the same energies at the parameter value $G = 0.375$, and with fitting of the depth of the potential weel by varying the parameter q, the values of which are given in Table 3.

The values v_j^i of the parameters for the ^{45}Fe nucleus and u_j^f for the ^{43}Cr nucleus are given in Tables 4-5.

Table 6 gives the values of the overlap coefficients G_{nlj}^{A} and G_{nlj}^{A-1}, as well as their products used in the calculations of the full and partial widths of the 2p decay of the ^{45}Fe nucleus for the shell levels $2p_{3/2}, 2p_{1/2}, 2s_{1/2}, 1d_{5/2}, 1d_{3/2}, 1f_{7/2}, 1f_{5/2}$. The values of correlation functions and chemical potentials λ_Z for ^{45}Fe, ^{44}Mn, and ^{43}Cr nuclei given in Table 7 lie within the range of values presented in [34].

The values of the total Γ and partial widths of the 2p decay of the ^{45}Fe nucleus calculated for the potentials [36-38] in the framework of the superfluid model of the atomic nucleus for the shell levels $2p_{3/2}, 2p_{1/2}, 2s_{1/2}, 1d_{5/2}, 1d_{3/2}, 1f_{7/2}, 1f_{5/2}$ and the values of the 2p decay energies Q_0 lying in the experimental range $Q_0 = (1.154 \pm 0.016)$MeV [18] are presented in Tables 8, 9. Table 9 shows that the widths of the levels $1d_{5/2}, 1d_{3/2}, 1f_{7/2}, 1f_{5/2}$ are more than 3 orders of magnitude smaller than the experimental value of the total 2p decay width $\Gamma^{\exp} = (1.6 \pm 0.5) \cdot 10^{-19}$MeV, and therefore they can be disregarded in the future. Tables 8, 9 show a strong dependence of the calculated widths on the choice of shell potentials [36-38] and energy values Q_0. The changes in the partial widths $\Gamma(2p_{3/2}), \Gamma(2p_{1/2}), \Gamma(2s_{1/2})$ and total width Γ are characterised by factors reaching values of 30, 27, 3,

Table 2. Energies (MeV) of proton shell levels of the ^{45}Fe nucleus calculated with the initial potentials [36-38] at q=1. with initial potentials [36-38] at q=1.

nlj	[36]	[37]	[38]
$1f_{5/2}$	3.5554	5.9963	5.7808
$2p_{1/2}$	3.3869	4.0703	4.6974
$2p_{3/2}$	2.9878	3.5070	3.8517
$1f_{7/2}$	1.8644	3.4647	2.3453
$2s_{1/2}$	−4.8655	−4.1695	−3.8399
$1d_{3/2}$	−6.8646	−4.8268	−5.2431
$1d_{5/2}$	−8.0278	−7.1723	−7.6657
$1p_{1/2}$	−16.9629	−16.2860	−16.1123
$1p_{3/2}$	−17.5382	−17.7372	−17.3060
$1s_{1/2}$	−25.7316	−27.0819	−25.6382

Table 3. Same as in Table 2, $q > 1$.

nlj	[36] q = 1.0058	[37] q = 1.0715	[38] q = 1.0195
$1f_{5/2}$	3.2143	4.2203	5.0746
$2p_{1/2}$	3.0037	2.6535	3.9827
$2p_{3/2}$	2.5830	2.0062	3.1514
$1f_{7/2}$	1.4258	1.4249	1.4784
$2s_{1/2}$	−5.5075	−6.6747	−4.9833
$1d_{3/2}$	−7.5201	−7.5314	−6.4631
$1d_{5/2}$	−8.7228	−9.9422	−8.9261
$1p_{1/2}$	−17.7913	−19.5716	−17.5984
$1p_{3/2}$	−18.3805	−21.0419	−18.7802
$1s_{1/2}$	−26.7873	−30.8798	−27.4175

Table 4. Coefficients for the ^{45}Fe core.

Potential	[36]	[37]	[38]
nlj	v_j	v_j	v_j
$1f_{5/2}$	0.293	0.276	0.219
$2p_{1/2}$	0.397	0.435	0.288
$2p_{3/2}$	0.461	0.555	0.394
$1f_{7/2}$	0.711	0.710	0.623
$2s_{1/2}$	0.991	0.994	0.993
$1d_{3/2}$	0.995	0.995	0.995
$1d_{5/2}$	0.996	0.997	0.997

Table 5. Coefficients for the ^{43}Cr core.

Potential	[36]	[37]	[38]
nlj	u_j	u_j	u_j
$1f_{5/2}$	0.980	0.980	0.979
$2p_{1/2}$	0.961	0.961	0.960
$2p_{3/2}$	0.933	0.932	0.931
$1f_{7/2}$	0.774	0.773	0.773
$2s_{1/2}$	0.125	0.125	0.125
$1d_{3/2}$	0.102	0.102	0.102
$1d_{5/2}$	0.079	0.079	0.076

CPC Accepted

Table 6. Overlap coefficients G^{A}_{nlj}, G^{A-1}_{nlj} and $G^{A}_{nlj}\cdot G^{A-1}_{nlj}$ calculated for potentials [36-38].

Potential	[36]			[37]			[38]		
nlj	G^{A}_{nlj}	G^{A-1}_{nlj}	$G^{A}_{nlj}\cdot G^{A-1}_{nlj}$	G^{A}_{nlj}	G^{A-1}_{nlj}	$G^{A}_{nlj}\cdot G^{A-1}_{nlj}$	G^{A}_{nlj}	G^{A-1}_{nlj}	$G^{A}_{nlj}\cdot G^{A-1}_{nlj}$
$1f_{5/2}$	0.718	0.980	0.704	0.676	0.980	0.662	0.536	0.979	0.525
$2p_{1/2}$	0.561	0.961	0.539	0.615	0.961	0.591	0.407	0.960	0.391
$2p_{3/2}$	0.922	0.933	0.860	1.110	0.932	1.035	0.788	0.931	0.734
$1f_{7/2}$	2.011	0.774	1.557	2.008	0.773	1.552	1.762	0.773	1.362
$2s_{1/2}$	1.401	0.125	0.175	1.406	0.125	0.176	1.410	0.125	0.176
$1d_{3/2}$	1.990	0.102	0.203	1.990	0.102	0.203	1.990	0.102	0.203
$1d_{5/2}$	2.440	0.079	0.193	2.442	0.079	0.193	2.442	0.076	0.186

Table 7. Values C_Z, λ_Z for ^{45}Fe, ^{44}Mn and ^{43}Cr.

Nucleus	Potential	C_Z, MeV	λ_Z, MeV
	[36]	1.850	1.200
^{45}Fe	[37]	1.755	1.194
	[38]	1.546	1.591
	[36]	1.608	1.522
^{44}Mn	[37]	1.747	1.113
	[38]	1.608	1.522
	[36]	1.682	1.026
^{43}Cr	[37]	1.698	1.005
	[38]	1.610	1.438

Table 8. Partial and total 2p decay widths of the ^{45}Fe nucleus.

Potential	Q_0, MeV	$\Gamma(2s_{1/2})10^{-19}$, MeV	$\Gamma(2p_{3/2})10^{-19}$, MeV	$\Gamma(2p_{1/2})10^{-19}$, MeV	$\Gamma 10^{-19}$ MeV
	1.138	0.041	0.381	0.072	0.495
[36]	1.154	0.055	0.505	0.096	0.657
	1.170	0.096	0.881	0.169	1.148
	1.138	0.027	1.182	0.128	1.337
[37]	1.154	0.036	1.566	0.170	1.772
	1.170	0.063	2.720	0.296	3.080
	1.138	0.031	0.093	0.008	0.131
[38]	1.154	0.041	0.123	0.011	0.175
	1.170	0.071	0.215	0.019	0.306

and 24 depending on the given choice.

Table 10 presents the ratios of partial widths $\Gamma(2p_{3/2})/\Gamma(2s_{1/2}), \Gamma(2p_{3/2})/\Gamma(2p_{1/2})$, and the ratio $\Gamma/\Gamma^{\rm exp}_{\rm min}\left(\Gamma/\Gamma^{\rm exp}_{\rm max}\right)$, where the values $\Gamma^{\rm exp}_{\rm min} = 1.1\cdot 10^{-19}$MeV and $\Gamma^{\rm exp}_{\rm max} = 2.1\cdot 10^{-19}$MeV correspond to the limits of the interval of the experimental values of the full width [18] given above.

Table 10 shows that the values of the calculated width G are close to the experimental values for the potentials [36-37], with the ratio $\Gamma/\Gamma^{\rm exp}_{\rm min}\left(\Gamma/\Gamma^{\rm exp}_{\rm max}\right)$ being equal to 1.04 (0.54) at $Q_0 = 1.170$MeV for the potential [36] and 1.20(0.62) at $Q_0 = 1.138$MeV for the potential [37], and the ratio of the widths varies $\Gamma(2p_{3/2})/\Gamma(2p_{1/2})$ in the range 5-12. Therefore, for the calculations of the angular distributions of protons emitted in the 2p decay of the ^{45}Fe nucleus in the next section, it is sufficient to consider only the amplitudes of the partial widths of the 2p decay. The ratio is 9.2 for the potential [36] and 43.8 for the potential [37] at the above energy values.

It should be emphasized that the variation of the parameter q within the range of 1- 1.07 and the superfluid parameters λ and Δ within the limits indicated in Table 1. VII, does not go beyond the standard procedure adopted in such calculations (see, e.g., [31, 32]). The values of λ and Δ for ^{45}Fe, ^{44}Mn and ^{43}Cr are in the intervals characteristic of this region of nuclei and are consistent with the results of Ref. [33]. Thus, the fitting is not arbitrary but rather amounts to matching of the microscopic parameters of the model with the known binding energies, which is a generally accepted method in nuclear physics. Moreover, the final agreement with the experimental width is achieved only with a well-defined combination of parameters, which indicates the predictive power of the formalism, rather than fitting to specific data.

V. ANGULAR DISTRIBUTION OF EMITTED PROTONS FOR TWO-PROTON DECAY OF A ^{45} FE NUCLEUS

Using the two-step two-proton decay formalism developed in Refs. [27-29] together with the superfluid nuclear model [34], we derive the angular distribution $W(\mathbf{k}_1,\mathbf{k}_2)$ of protons emitted in the ground-state two-proton decay of ^{45}Fe leading to the ground state of ^{43}Cr. The distribution depends on the wave vectors $\mathbf{k}_1$ and $\mathbf{k}_2$ of the first and second emitted protons, whose directions in the laboratory frame are specified by the solid angles $\Omega_{\mathbf{k}_1}$ and $\Omega_{\mathbf{k}_2}$.

CPC Accepted

Table 9. Partial widths of the 2p decay of the ^{45}Fe nucleus.

Potential	Q_0, MeV	$\Gamma(1d_{5/2})$, MeV	$\Gamma(1d_{3/2})$, MeV	$\Gamma(1f_{7/2})$, MeV	$\Gamma(1f_{5/2})$, MeV
	1.138	0.987·10-24	0.109·10'23	0.240·10-22	0.362·10-24
[36]	1.154	0.132·10-23	0.146·10'23	0.318·10-22	0.486·10-24
	1.170	0.233·10-23	0.258·10'23	0.550·10-22	0.862·10'24
	1.138	0.649·10-24	0.681·10'24	0.144·10-22	0.690·10'25
[37]	1.154	0.869·10-24	0.911·10'24	0.190·10-22	0.925·10'25
	1.170	0.154·10−23	0.161·10−23	0.329·10−22	0.164·10'24
	1.138	0.639·10−24	0.706·10−24	0.187·10−22	0.169·10'25
[38]	1.154	0.855·10−24	0.944·10−24	0.248·10−22	0.227·10'25
	1.170	0.151·10−23	0.166·10−23	0.430·10'22	0.405·10'25

Table 10. Values of the ratios $\Gamma(2p_{3/2})/\Gamma(2s_{1/2})$, $\Gamma(2p_{3/2})/\Gamma(2p_{1/2})$, $\Gamma/\Gamma^{\rm exp}_{\rm min}(\Gamma/\Gamma^{\rm exp}_{\rm max})$ for the 2p decay of the 45Fe nucleus.

Potential	Q_0, MeV	$\Gamma(2p_{3/2})/\Gamma(2s_{1/2})$	$\Gamma(2p_{3/2})/\Gamma(2p_{1/2})$	$\Gamma/\Gamma^{\rm exp}_{\rm min}$	$\Gamma/\Gamma^{\rm exp}_{\rm max}$
	1.138	9.29	5.29	0.45	0.23
[36]	1.154	9.18	5.26	0.60	0.31
	1.170	9.18	5.21	1.04	0.54
	1.138	43.78	9.23	1.20	0.62
[37]	1.154	43.50	9.21	1.61	0.84
	1.170	43.17	9.19	2.8	1.46
	1.138	3.00	11.63	0.12	0.06
[38]	1.154	3.00	11.18	0.16	0.08
	1.170	3.03	11.32	0.28	0.14

Assuming that the emitted proton pair forms a singlet state with total spin $(S=0)$, which provides the dominant contribution to the decay, the normalized angular distribution is given by

$$W(\mathbf{k}_1,\mathbf{k}_2)=\frac{1}{\Gamma}\left|\sum_{lm}\sqrt{\frac{\Gamma(nlj_l)}{2l+1}}Y_{lm_l}(\Omega_{\mathbf{k}_1})Y_{l-m_l}(\Omega_{\mathbf{k}_2})\right|^2 \quad (60)$$

where $\sqrt{\Gamma(nlj_l)}$ denotes the partial decay amplitude corresponding to the emission of the first proton with orbital angular momentum and the second proton with orbital angular momentum. The amplitudes associated with the dominant partial widths obtained in Sec. IV are retained in the calculation.

To simplify the analysis, we introduce a coordinate system in which the Z' -axis is chosen along the momentum of the first emitted proton. In this frame, the spherical harmonics are transformed accordingly, while the polar angle of the first proton becomes zero. The direction of the second proton $\mathbf{k}_2$ is then completely determined by the opening angle $\Omega_{\mathbf{k}_2,\mathbf{k}_1}$ between the two emitted protons.

Using the transformation

$$Y_{lm_l}(0)=\sqrt{\frac{2l+1}{4\pi}}\delta_{m_l,0} \quad (61)$$

and integrating over the direction of the first proton, Eq. (60) reduces to

$$W(\theta)=\frac{1}{\Gamma}\left|\sum_{l}\sqrt{\Gamma(nlj_l)}Y_{l0}(\theta)\right|^2 \quad (62)$$

where $\theta=\theta_{\mathbf{k}_2,\mathbf{k}_1}$ is the angle between the directions of the vectors $\mathbf{k}_2$ and $\mathbf{k}_1$. From (62), the normalized angular distribution is obtained as

$$\bar{W}(\theta)=\frac{2\pi}{\Gamma}\sum_{ll'}\sqrt{\Gamma(nlj_l)}\sqrt{\Gamma(nl'j_{l'})}Y_{l0}(\theta)Y_{l'0}(\theta)\sin\theta \quad (63)$$

subject to the normalization condition

$$\int_0^\pi \bar{W}(\theta)d\theta=1 \quad (64)$$

The representation (63) is particularly convenient because it can be compared directly with the experimentally measured unit-normalized angular distributions $\bar{W}^{\rm exp}(\theta)$ reported in Refs. [20, 21, 40]. The corresponding experimental distribution is shown in Fig. 3(a).

The symmetry properties of the spherical harmonics $Y_{l0}(\theta)$,

$$Y_{l0}(\theta)=(-1)^l Y_{l0}(\pi-\theta) \quad (65)$$

show that a symmetric angular distribution is expected when only partial waves of identical parity contribute. Consequently, the experimentally observed asymmetry of

CPC Accepted

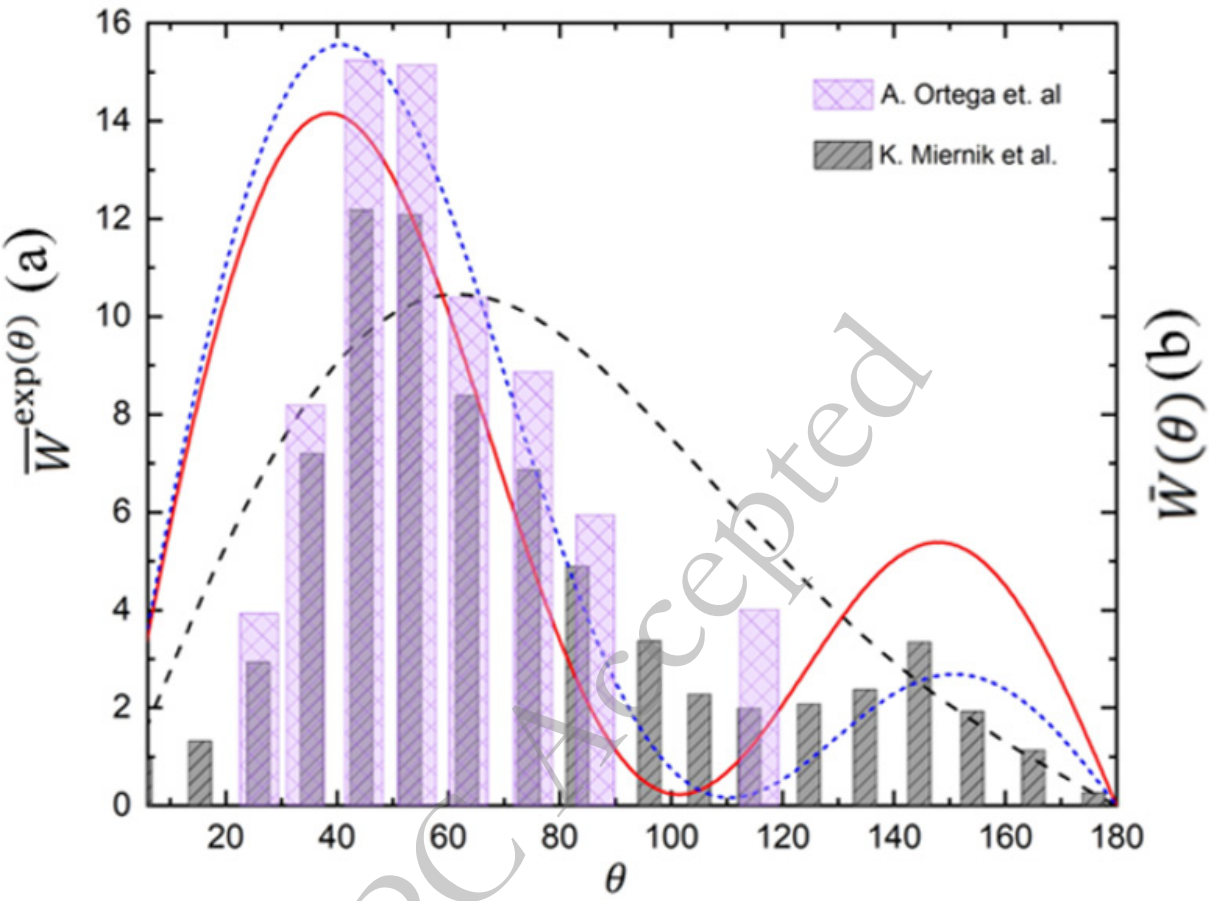

CPC Accepted

Fig. 3. (a). Unit-normalised experimental [21, 40] angular distribution $\bar{W}^{\exp}(\theta)$ of protons - products of the 2p decay of the ^{45}Fe nucleus, presented as a histogram. (b) Comparison of the experimental [21, 40] $\bar{W}^{\exp}(\theta)$ (histogram) and calculated by formulas (66)$\bar{W}(\theta)$ at different values of the fitted parameter β_0 : dashed-dotted curve -$\beta_0 = 0.21$; dotted curve $-\beta_0 = 1.7$; solid curve is $\beta_0 = 3$.

the proton angular distribution can only arise from the interference between decay amplitudes corresponding to orbital angular momenta of opposite parity.

Retaining only the dominant partial widths $\Gamma(2p_{3/2})$ and $\Gamma(2s_{1/2})$ identified in the previous section and introducing the ratio $\beta^2 = \Gamma(2p_{3/2})/\Gamma(2s_{1/2})$, Eq. (63) can be reduced to the one-parameter expression

$$\bar{W}(\theta) = \frac{1}{2(1+\beta^2)}\left(1+\sqrt{3}\beta\cos\theta\right)^2\sin\theta \qquad (66)$$

To analyse the possibility of describing by the one-parameter expression (66) the experimental angular distribution of protons $\bar{W}^{\exp}(\theta)$ [20-21], we use the fitting method [39]. The calculations show that the minimal deviations $\bar{W}^{\exp}(\theta)$ from $\bar{W}(\theta) = \text{are}\beta = \beta_0 = 0.21; 1.7; 3$.

A comparison of the calculated values $\beta = \sqrt{\Gamma(2p_{3/2})/\Gamma(2s_{1/2})}$ (Table 10) and the value $\beta_0 = 0.21$ leads to the conclusion that in the intervals of experimental values of both the 2p decay energy $Q_0 = (1.154 \pm 0.016)$MeV and the total decay width $\Gamma^{\exp} = (1.6 \pm 0.5)\cdot 10^{-19}$MeV for all three sets of parameters of the considered shell potentials [36-38], the indicated value β_0 does not agree with the calculated values β. The agreement of $\beta_0 = 1.7$ with the corresponding values is present only for the potential [38]. But for this potential the calculated value of the total width Γ differs from its experimental value by a factor greater than 4, so that $\beta_0 = 1.7$ can also be excluded from consideration. Finally, $\beta_0 = 3$ reasonably agrees with the values of β (Table 10) only for the potential [36] at the upper limit of the 2p decay energy = 1.17MeV and the lower limit of the experimental width $\Gamma^{\exp}_{\min} = 1.1\cdot 10^{-19}$MeV. The comparison of the normalised angular distribution $\bar{W}(\theta)$ at $\beta_0 = 3$ and the experimental $\bar{W}^{\exp}(\theta)$, shown in FIG. 3(b), demonstrates their qualitative agreement.

To enable a meaningful comparison between the unit-normalized theoretical probability density $\bar{W}(\theta)$ and the experimental data, the calculated curves were multiplied by an overall scaling factor. This factor accounts for the total number of recorded experimental events and the angular bin width of 10°. As a result of this standard normalization procedure, the theoretical curve for $\beta_0 = 3$ not only automatically reproduces the experimental amp-

litude of 14-16 counts in the primary peak region ($\theta = 40°$), but also accurately describes the overall shape of the entire angular distribution.

Finally, the combined analysis of the total decay width presented in Sec. IV and the angular distribution considered here indicates that only the shell-model potential of Ref. [36] provides a simultaneous description of both observables within the experimental uncertainties. This result demonstrates the strong sensitivity of two-proton radioactivity to the underlying single-particle potential and confirms that the angular correlation of the emitted protons provides an additional and independent constraint on the microscopic description of the decay mechanism.

VI. CONCLUSION

In the present work, a general quantum-mechanical theory of two-step two-proton decay has been developed on the basis of the multiparticle formalism of one-proton radioactivity. The theory takes strict account of pairing and superfluid correlations of nucleons in the parent (Z, A), intermediate (Z-1, A-1), and final (Z-2, A-2) nuclei. The proposed approach describes two-proton emission as two successive one-proton transitions connected by the Green's function of the intermediate nucleus and provides a unified treatment of both sequential and virtual decay mechanisms within a single theoretical framework.

Unlike conventional quasiclassical approaches, the present formalism is derived entirely within quantum mechanics and does not require the introduction of channel radii. Since the theory is formulated in terms of microscopic one-proton decay amplitudes, it consistently incorporates the nuclear structure of the initial, intermediate, and final nuclei, including shell structure, angular-momentum coupling, pairing correlations, and superfluid effects. Consequently, the formalism can be applied to both spherical and deformed nuclei as well as to diagonal and, for spherical nuclei, off-diagonal one-proton transitions.

The derived expressions for the sequential and virtual two-proton decay widths naturally arise from the same Green-function formalism. The sequential contribution reduces to the well-established results of the R -matrix theory [11] and the kinetic-equation approach [12], providing an important consistency check of the present formulation. At the same time, the virtual contribution extends the theoretical description to off-shell intermediate configurations within the same microscopic framework.

The developed formalism has been applied to the ground-state two-proton decay of ^{45}Fe leading to the ground state of ^{43}Cr. Numerical calculations performed within the superfluid nuclear model demonstrate a pronounced dependence of the calculated total and partial decay widths on the choice of the single-particle shell potential. Among the potentials considered in the present work, the parameterization of Ref. [36] provides the only simultaneous description of both the experimental total decay width and the measured proton angular distribution.

This is justified by the fact that in the energy range under consideration (about 1MeV) and for nuclei with a sufficiently large charge ($Z = 26$), the Coulomb repulsion between protons makes a correction of the order of several percent to the full width, which is significantly less than the observed sensitivity to the choice of a single-particle potential (which reaches a factor of 10-20). In the sequential channel, the interaction between protons is suppressed because of the time separation between the emissions. For a virtual channel, the inclusion of the proton-proton Coulomb interaction would require a modification of the three-particle Green-function, which is beyond the scope of this work, but can be considered in the future as a development of formalism. Nevertheless, the good agreement with experiment suggests that neglecting this interaction is a reasonable first approximation.

CPC Accepted

ACKNOWLEDGEMENTS

The authors express their gratitude to the blessed memory of Yuri Vladimirovich Ivan kov, Associate Professor of the Department of Nuclear Physics, whose many years of contributions to the study of two-proton decay of nuclei have become the foundation f or the development of this research direction. The scientific ideas and methodological approaches of Yu.V. Ivankov remain relevant and continue to serve as a guiding refer ence for researchers in the field of nuclear physics.

References

[1] P. I. Woods and C. N. Davids, Annu. Rev. Nucl. Part. Sci. **47**, 54 (1997)
[2] S. G. Kadmensky and V. E. Kalechits, Yad. Fiz. **12**, 70 (1970)
[3] S. G. Kadmensky and V. I. Furman, Alpha Decay and Related Nuclear Reactions (Energoatomizdat, Moscow, 1985).
[4] S. G. Kadmensky and V. G. Khlebostroev, Yad. Fiz. **18**, 980 (1973)
[5] V. P. Bugrov, S. G. Kadmensky, and V. I. Furman, Yad. Fiz. **41**, 1123 (1985)
[6] V. P. Bugrov, V. E. Bunakov, S. G. Kadmensky, and V. I. Furman, Yad. Fiz. **42**, 57 (1985)
[7] V. P. Bugrov and S. G. Kadmensky, Yad. Fiz. **49**, 1562 (1989)
[8] V. I. Goldansky, Nucl. Phys. **19**, 482 (1960)

[9] L. V. Grigorenko, Phys. Part. Nucl. **40**, 1277 (2009)
[10] S. G. Kadmensky, Phys. At. Nucl. **68**, 184 (2005)
[11] A. M. Lane and A. G. Thomas, Rev. Mod. Phys. **30**, 257 (1958)
[12] E. Segre, Experimental Nuclear Physics, Vol. 3 (IIL, Moscow, 1961), p. 13.
[13] L. V. Grigorenko, R. C. Johnson, and I. G. Mukha, *et al*., Phys. Rev. Lett. **85**, 22 (2000)
[14] L. V. Grigorenko, R. C. Johnson, and I. G. Mukha, *et al*., Phys. Rev. C **64**, 054002 (2001)
[15] L. V. Grigorenko and M. V. Zhukov, Phys. Rev. C **76**, 014009 (2007)
[16] V. I. Goldansky, Sov. Phys. Usp. **8**, 770 (1966)
[17] M. Pfützner, E. Badura, and C. Bingham, *et al*., Eur. Phys. J. A **14**, 279 (2002)
[18] J. Giovinazzo, B. Blank, and M. Chartier, *et al*., Phys. Rev. Lett. **89**, 102501 (2002)
[19] C. Dossat, A. Bey, and B. Blank, *et al*., Phys. Rev. C **72**, 054315 (2005)
[20] K. Miernik, W. Dominik, and Z. Janas, *et al*., Phys. Rev. Lett. **99**, 192501 (2007)
[21] K. Miernik, *et al*., Nucl. Instrum. Methods Phys. Res. A **581**, 194 (2007)
[22] B. A. Brown and F. C. Barker, Phys. Rev. C **67**, 041304(R) (2003)
[23] L. D. Landau and Ya. A. Smorodinsky, Zh. Eksp. Teor. Fiz. **14**, 269 (1944)
[24] A. B. Migdal, Zh. Eksp. Teor. Fiz. **28**, 3 (1955)
[25] K. M. Watson, Phys. Rev. **88**, 1163 (1952)
[26] L. V. Grigorenko, Phys. Part. Nucl. **40**, 1273 (2009)
[27] S. G. Kadmensky and Yu. V. Ivankov, Yad. Fiz. **77**, 1075 (2014)
[28] S. G. Kadmensky and Yu. V. Ivankov, Yad. Fiz. **77**, 1605 (2014)
[29] S. G. Kadmensky and Yu. V. Ivankov, Izv. RAN, Ser. Fiz. **78**, 1414 (2014)
[30] Buck B., Merchant A. C. Phys. Rev. C **39**, 2097 (1989)
[31] V. P. Bugrov, S. G. Kadmensky, V. I. Furman, and V. G. Khlebostroev, Yad. Fiz. **41**, 1123 (1985)
[32] Pfützner M., Grigorenko L. V., Karny M., Riisager K. Rev. Mod. Phys. **84**, 567 (2012)
[33] J. Rotureau, J. Okołowicz, and M. Płoszajczak, Nucl. Phys. A **767**, 13 (2006)
[34] V. G. Soloviev, Theory of Atomic Nucleus: Nuclear Models (Energoatomizdat, Moscow, 1981).
[35] A. B. Migdal, Theory of Finite Fermi Systems and Properties of Atomic Nuclei (Nauka, Moscow, 1965).
[36] S. A. Fayans, Preprint IAE-1593 (1968).
[37] F. D. Becchetti and G. W. Greenlees, Phys. Rev. **182**, 1190 (1969)
[38] P. E. Nemirovsky, Modern Models of the Atomic Nucleus (Atomizdat, Moscow, 1980).
[39] G. Cramer, Mathematical Methods of Statistics (Mir, Moscow, 1975).
[40] A. Ortega Moral, S. M. Wang, and J. Giovinazzo, *et al*., Phys. Rev. C **112**, L061302 (2025)

CPC Accepted